SUPPLEMENTARY MATERIAL

Solan M, Ward ER, Wood CL, Reed AJ, Grange LJ, Godbold JA
Climate driven benthic invertebrate activity and biogeochemical functioning across the Barents Sea Polar Front
Phil. Trans. Roy. Soc. A (doi.org/10.1098/rsta.2019.0365)

Data availability

All data used to generate this manuscript are openly available from the Discovery Metadata System (https://www.bas.ac.uk/project/dms/), a data catalogue hosted by The UK Polar Data Centre (UK PDC, https://www.bas.ac.uk/data/uk-pdc/). These data supported the present manuscript:

Solan, M., Godbold, J., Grange, L., Ward, E. R., Wood, C., & Reed, A. (2020). Experimental measurements for replicate macrofaunal communities from the Western Barents Sea for summer 2017 and 2018 (Version 1.0) [Data set]. UK Polar Data Centre, Natural Environment Research Council, UK Research & Innovation. https://doi.org/10.5285/62A44C8D-5593-4D2C-93D9-5DDFEBCBFC36

Solan, M., Godbold, J., Grange, L., Ward, E. R., Wood, C., & Reed, A. (2020). Fluorescent sediment profile images (fSPI) for replicate macrofaunal communities from the Western Barents Sea for summer 2017 and 2018 (Version 1.0) [Data set]. UK Polar Data Centre, Natural Environment Research Council, UK Research & Innovation. https://doi.org/10.5285/82771E90-65D6-4F56-B766-A16FE099FC98

Solan, M., Godbold, J., Grange, L., Ward, E. R., Wood, C., & Reed, A. (2020). Sediment surface images (SSI) for replicate macrofaunal communities from the Western Barents Sea for summer 2018 (Version 1.0) [Data set]. UK Polar Data Centre, Natural Environment Research Council, UK Research & Innovation. https://doi.org/10.5285/B62AF357-CBEE-4A98-894B-5ED3C11CEF7D

Solan, M., Godbold, J., Grange, L., Ward, E. R., Wood, C., & Reed, A. (2020). Vertical luminophore particle tracer profiles expressed as relative counts for replicate macrofaunal communities from the Western Barents Sea in summer 2017 and 2018 (Version 1.0) [Data set]. UK Polar Data Centre, Natural Environment Research Council, UK Research & Innovation. https://doi.org/10.5285/260B15B1-F814-4941-84CD-9CD94F386F33

Solan, M., Godbold, J., Grange, L., Ward, E. R., Wood, C., & Reed, A. (2020). Macrofaunal abundance and biomass for replicate macrofaunal communities from the Western Barents Sea for summer 2017 and 2018 (Version 1.0) [Data set]. UK Polar Data Centre, Natural Environment Research Council, UK Research & Innovation. https://doi.org/10.5285/7FBCA0A1-E2C1-4265-A7A5-713451CB52C0

Solan, M., Godbold, J., Grange, L., Ward, E. R., Wood, C., & Reed, A. (2020). Sediment organic material by loss on ignition for stations from the Western Barents Sea for summer 2017 and 2018 (Version 1.0) [Data set]. UK Polar Data Centre, Natural Environment Research Council, UK Research & Innovation. https://doi.org/10.5285/24BE3CC9-4F49-4812-99CE-2F6668541E98

Solan, M., Godbold, J., Grange, L., Ward, E. R., Wood, C., & Reed, A. (2020). Sediment particle size analysis for stations from the Western Barents Sea for summer 2017 and 2018 (Version 1.0) [Data set]. UK Polar Data Centre, Natural Environment Research Council, UK Research & Innovation. https://doi.org/10.5285/C6285ED6-0A44-4115-8F7C-C099B9B358EA

Cruise reports for this research programme can be obtained from the British Oceanographic Data Centre at:
https://www.bodc.ac.uk/resources/inventories/cruise_inventory/results/
Cottier FR. 2017 RRS James Clark Ross cruise, JR16006
Solan M. 2018 RRS James Clark Ross cruise, JR17007
Barnes D. 2019 RRS James Clark Ross cruise, JR18006 (not relevant to the present manuscript, but listed here as it forms the third and final cruise of this research programme).

Figure S1. The daily sea ice extent values for 2nd December 2014 to 28th January 2020 at 1km grid cell size resolution for the Barents Sea region obtained from the Multisensor Analyzed Sea Ice Extent (MASIE) product (https://nsidc.org/data/G02186/versions/1; Fetterer et al. 2010) at the National Snow and Ice Data Center (http://nsidc.org/). Years are indicated by colour (2014, black; 2015, red; 2016, green; 2017, blue; 2018, cyan; 2019, magenta; 2020, yellow). The period of station occupancy for research cruise JCR16006 in 2017, and JCR17007 in 2018, are indicated (grey horizontal bars).

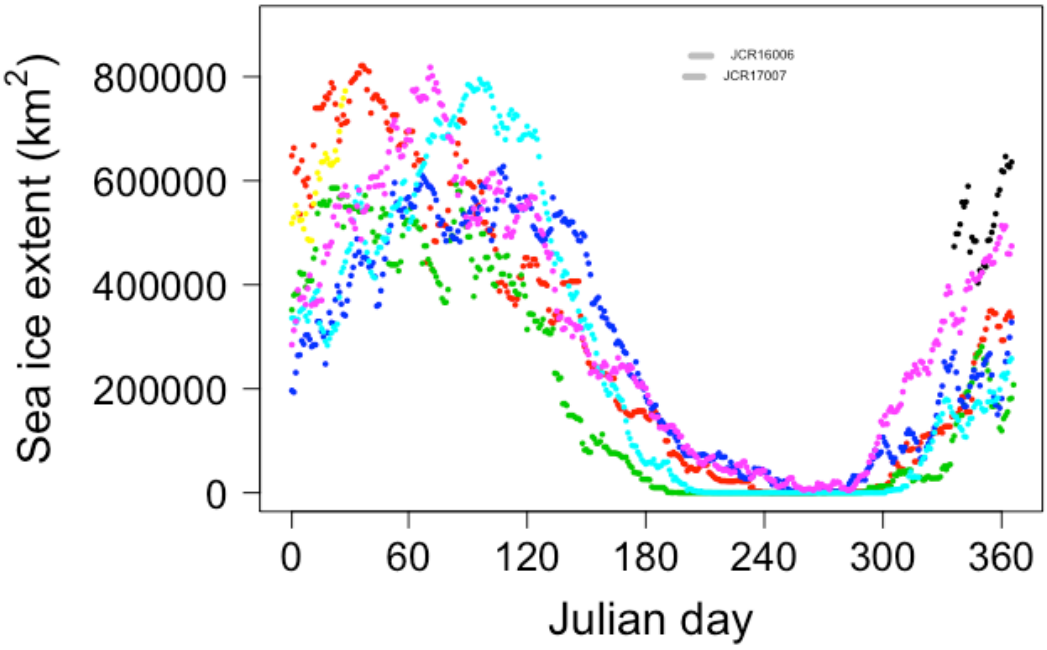

Table S1: Summary of the geographical position, water column depth and timing of each box core obtained for this study during research cruises JCR16006 and JCR17007, RRS James Clark Ross. Each deployment of the box core is associated with a cruise event number from the ship log. Timings refer to the ship position at the point of bottom contact during box core deployment.

Cruise	Station	Event number	Latitude (N)	Longitude (E)	Depth (m)	Time (UTC) and date at bottom
JCR16006	B13	331	74.49999	29.99977	359	02:38, 01 August 2017
		332	74.50018	29.99978	359	03:06, 01 August 2017
		333	74.50019	30.00041	359	03:33, 01 August 2017
		334	74.50003	30.00036	358	04:03, 01 August 2017
JCR16006	B14	318	76.50033	30.50090	293	03:08, 31 July 2017
		319	76.50030	30.50174	293	03:34, 31 July 2017
		320	76.50011	30.50173	294	04:02, 31 July 2017
		321	76.49993	30.50174	294	04:27, 31 July 2017
JCR16006	B15	286	78.25026	30.00207	314	14:14, 29 July 2017
		287	78.25015	30.00227	313	14:34, 29 July 2017
		288	78.25004	30.00212	313	14:54, 29 July 2017
		289	78.24998	30.00209	313	15:14, 29 July 2017
JCR16006	B16	200	80.11071	30.03578	286	19:42, 22 July 2017
		201	80.11678	30.06457	281	20:13, 22 July 2017
		203	80.10758	30.03939	288	21:50, 22 July 2017
		205	80.11099	30.07918	280	22:43, 22 July 2017
JCR16006	B17	227	81.27498	29.26483	335	16:25, 24 July 2017
		228	81.27642	29.24559	335	16:57, 24 July 2017
		229	81.27892	29.23538	332	17:23, 24 July 2017
		230	81.28249	29.23142	326	17:50, 24 July 2017
JCR17007	B13	289	74.50010	29.99813	358	06:40, 28 July 2018
		291	74.50028	29.99748	359	07:40, 28 July 2018
		292	74.50008	29.99748	360	08:08, 28 July 2018
		293	74.49990	29.99755	359	08:38, 28 July 2018
JCR17007	B14	237	76.49917	30.49924	293	15:48, 25 July 2018
		238	76.49923	30.49987	294	16:13, 25 July 2018
		239	76.49925	30.50065	294	16:40, 25 July 2018
		240	76.49940	30.50113	296	17:06, 25 July 2018
JCR17007	Xs	270	77.03279	29.33267	228	05:04, 27 July 2018
		271	77.03288	29.33338	229	05:27, 27 July 2018
		272	77.03290	29.33407	230	05:50, 27 July 2018
		273	77.03305	29.33449	235	06:13, 27 July 2018
JCR17007	B15	205	78.25151	30.00001	317	08:04, 24 July 2018
		206	78.25149	29.99928	318	08:32, 24 July 2018
		207	78.25161	29.99843	318	09:01, 24 July 2018
		208	78.25142	29.99809	319	09:32, 24 July 2018
JCR17007	B16	189	80.11620	30.06719	283	09:13, 23 July 2018
		190	80.11618	30.06817	285	09:39, 23 July 2018
		191	80.11634	30.06881	279	10:04, 23 July 2018
		192	80.11642	30.06969	280	10:35, 23 July 2018
JCR17007	B17	134	81.28105	29.32781	337	04:45, 19 July 2018
		135	81.28124	29.32828	337	05:15, 19 July 2018
		136	81.28133	29.32941	337	05:43, 19 July 2018
		137	81.28136	29.32802	345	06:13, 19 July 2018

Figure S2: Study area indicating (a) the position of stations B13-B17 and Xs, the bathymetry relative to chart datum and the generally accepted approximate position of the oceanographic (black) and benthic (grey) polar front. In (b), the position of each replicate box core (n = 4 station^{-1} year^{-1}: 2017, black; 2018, red) shows good agreement in site occupancy.

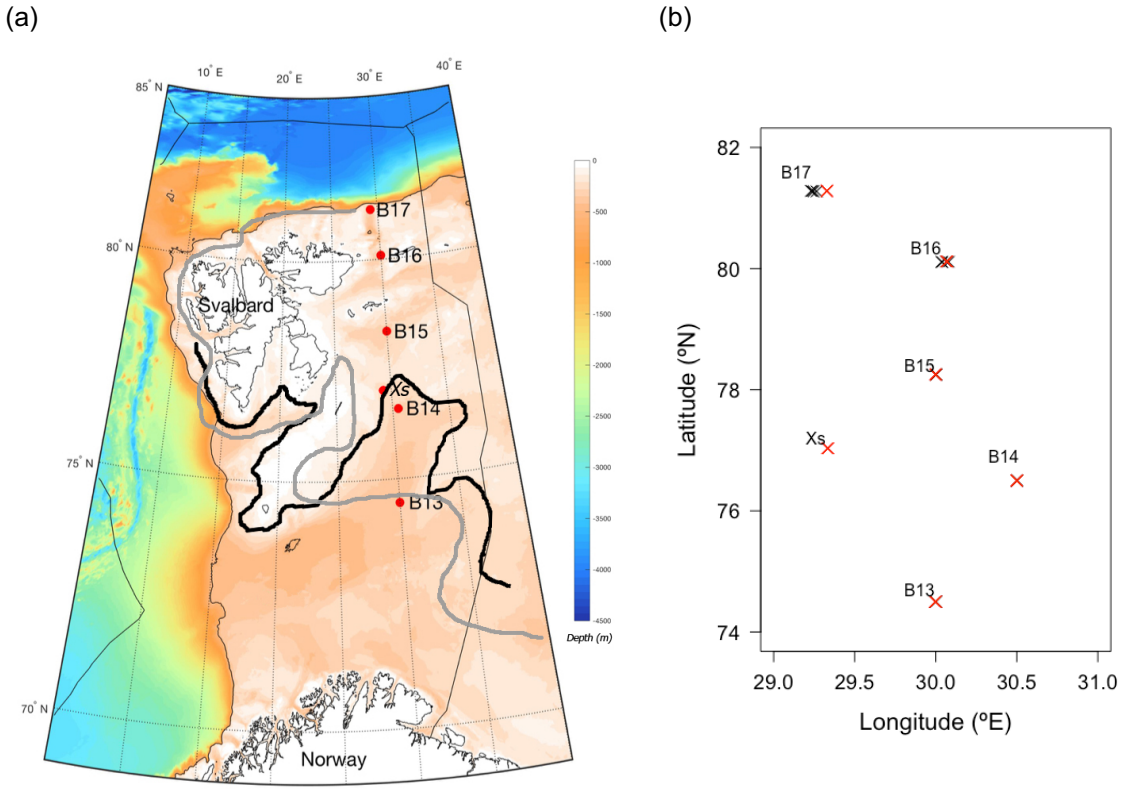

Figure S3: Retrieval of each intact core (LWH: 20 × 20 × 12 cm) obtained from (a) each of four replicate 0.1m^2 USNL (Unites States Naval Laboratory) box cores using a core extruder and (b-c), transferral to transparent acrylic aquaria (internal dimensions, LWH: 20 × 20 × 34 cm).

Figure S4: System of (a) interconnected insulated fibreglass seawater baths (lids removed, LWH: 1.2 x 1.2 x 0.8m) used to house the intact cores (retrieved as per Figure S3), with temperature controlled by a chiller (located top left of (a)). In each seawater bath, each aquarium was allocated a position randomly and (b) was continually aerated by bubbling through a glass pipette linked to a controllable air supply fed through the grey ducting. The green coloration in each aquarium are the luminophores used to track infaunal particle mixing.

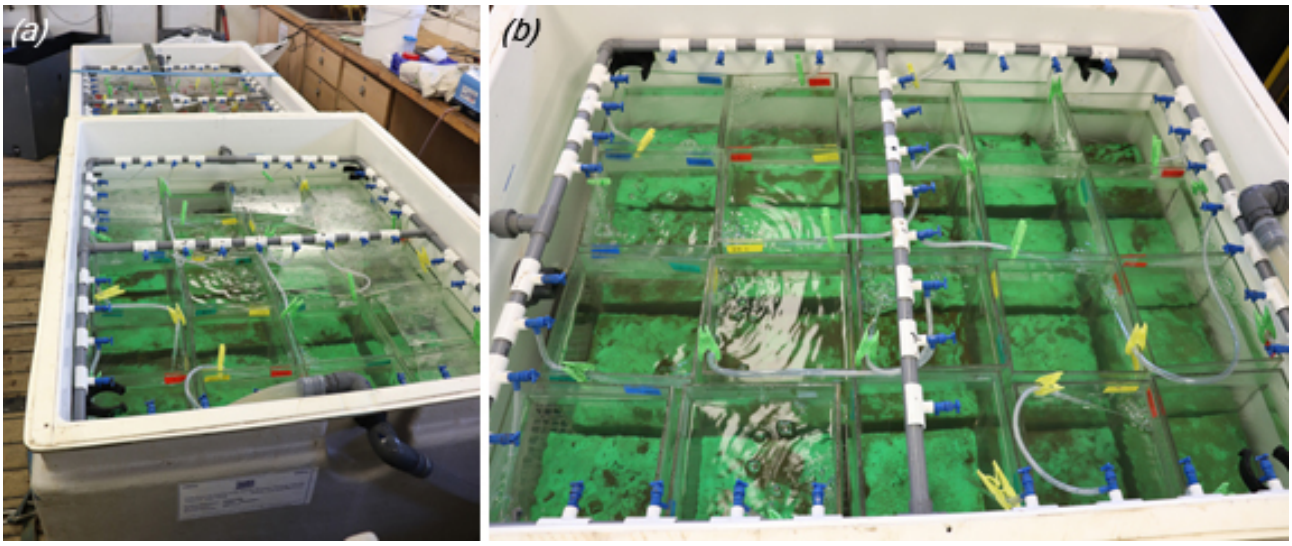

Table S2: The near bottom water temperatures from the proximate CTD (conductivity, temperature, depth) casts taken at each station. Data courtesy of Dr. Sian Henley, University of Edinburgh.

Station	**Latitude (N)**	**Longitude (E)**	**Depth (m)**	**Bottle depth (m)**	**Temperature #1 (°C)** (mean ± s.d.)	**Temperature #2 (°C)** (mean ± s.d.)	**Time (UTC) and date (*ddmmyy*)**
JCR16006							
B13	74.4998	29.9982	346	345.7	2.418	2.418	01:27, 01/08/17
B14	76.4463	29.3272	243	231.6	1.444	1.44	11:04, 31/07/17
B15	78.2503	30.0073	316	299.3	-1.442	-1.439	13:19, 29/07/17
B16	80.1513	29.9146	294	277.6	-1.436	-1.438	08:02, 22/07/17
B17	81.4017	29.5033	291	278.0	1.756 (0.548±1.848)	1.752 (0.547±1.846)	08:00, 25/07/17
JCR17007							
B13	74.5000	30.0002	357	350.6	0.802	0.801	03:54, 28/07/18
B14	76.5000	30.5003	292	284.3	1.533	1.532	01:53, 25/07/18
Xs	77.0333	29.3335	228	219.6	1.452	1.451	16:51, 26/07/18
B15	78.2517	30.0002	313	303.1	-0.554	-0.546	11:37, 16/07/18
B16	80.1167	30.0683	280	270.6	0.387	0.386	10:18, 22/07/18
B17	81.2816	29.3269	334	327.5	0.982 (0.767±0.774)	0.981 (0.768±0.771)	06:37, 18/07/18

Figure S5: Replicate (n=4) f-SPI images for (a) 2017 and (b) 2018 from station B13. The images (four aquarium sides are stitched together) are presented. The green coloration is the luminophore tracer.

(a)

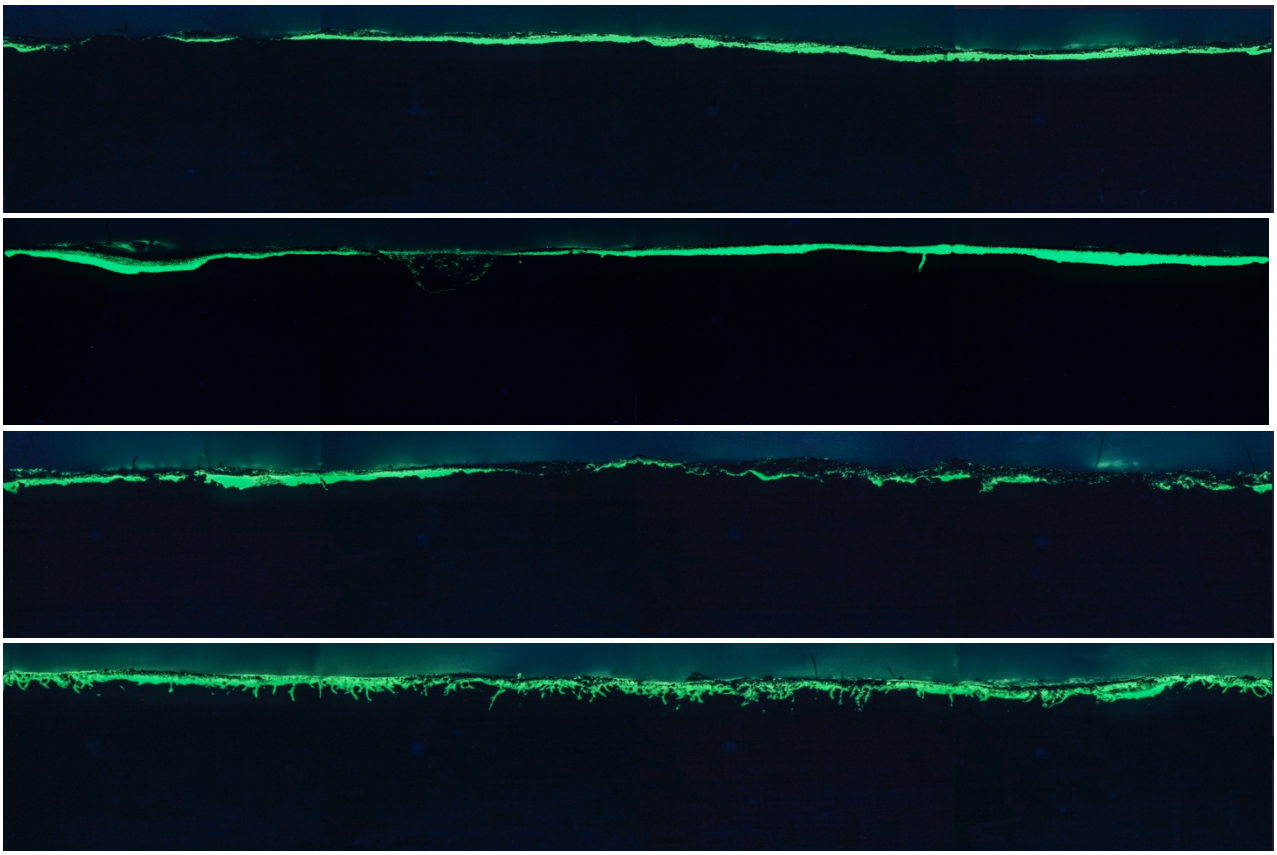

(b)

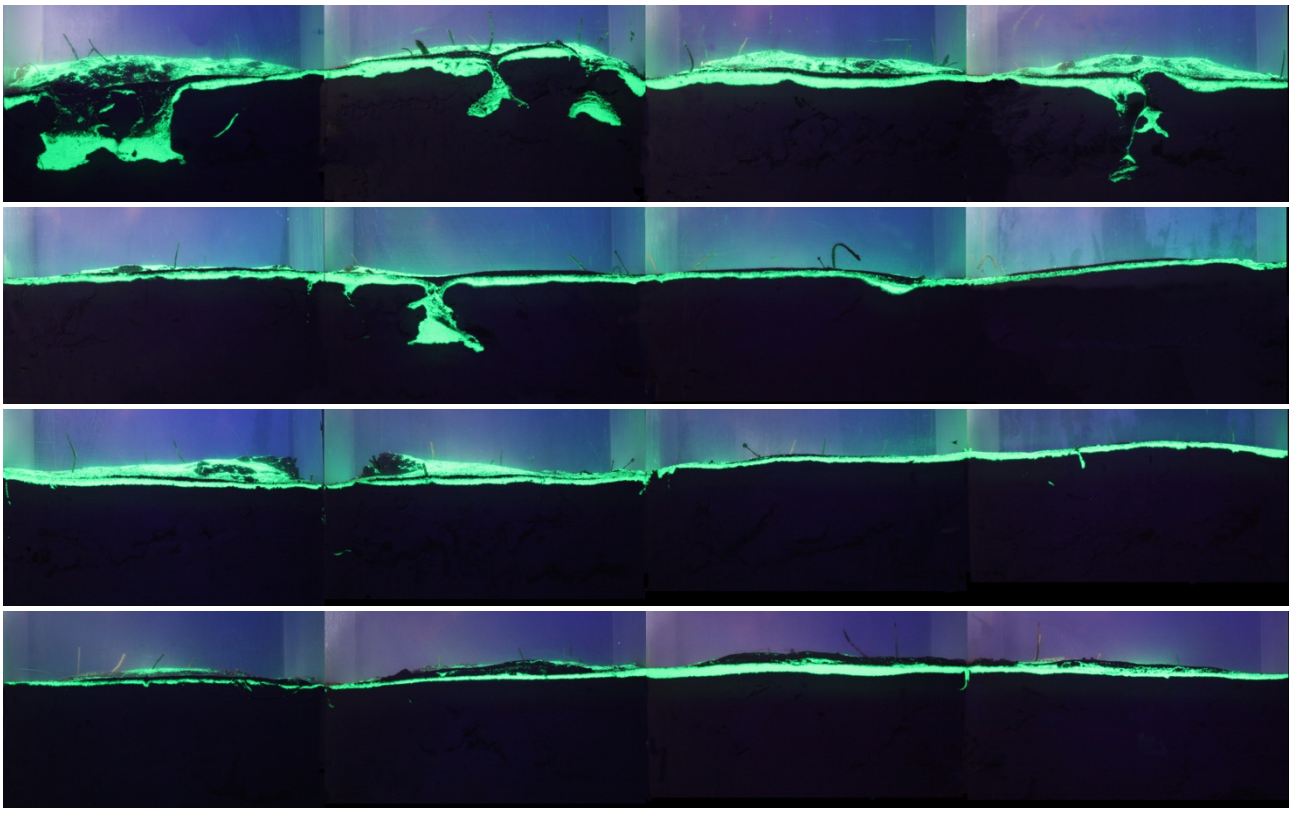

Figure S6: Replicate (n=4) f-SPI images for (a) 2017 and (b) 2018 from station B14. The images (four aquarium sides are stitched together) are presented. The green coloration is the luminophore tracer.

(a)

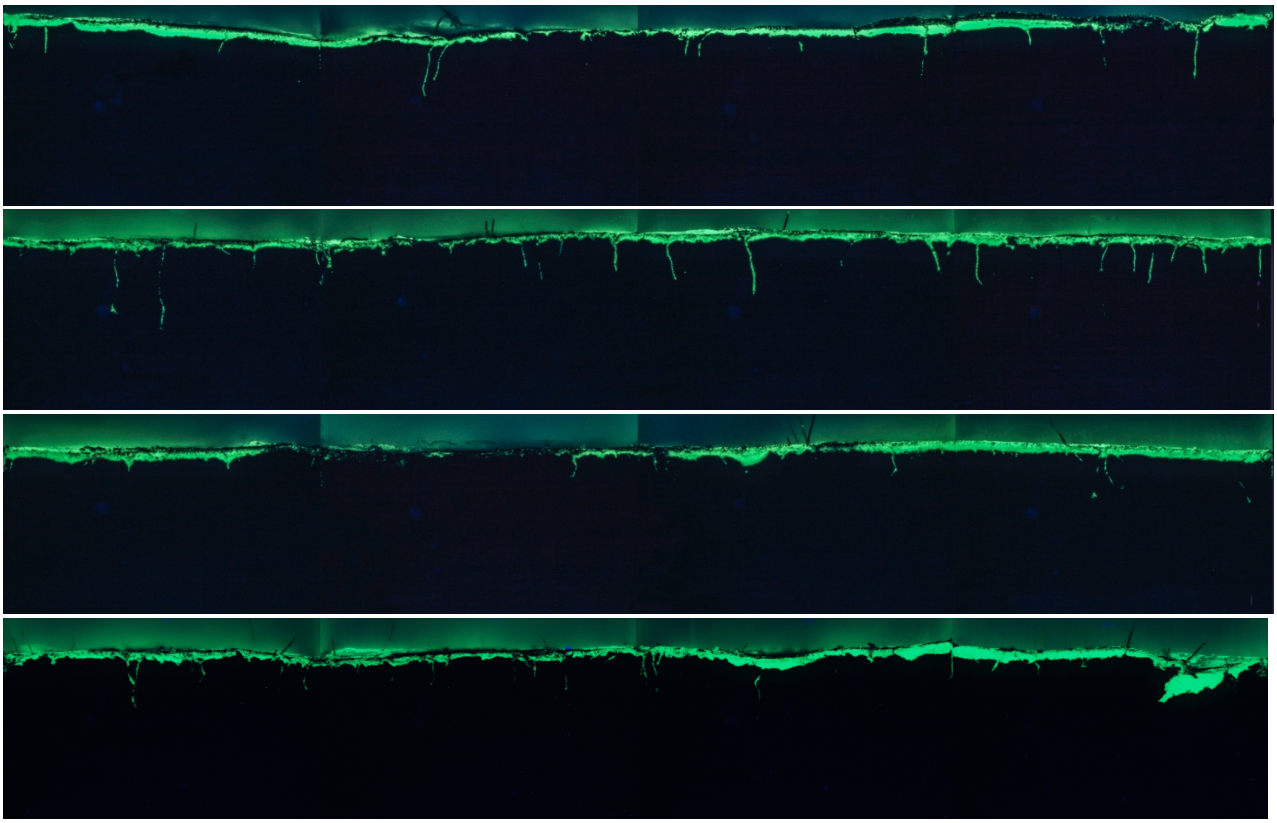

(b)

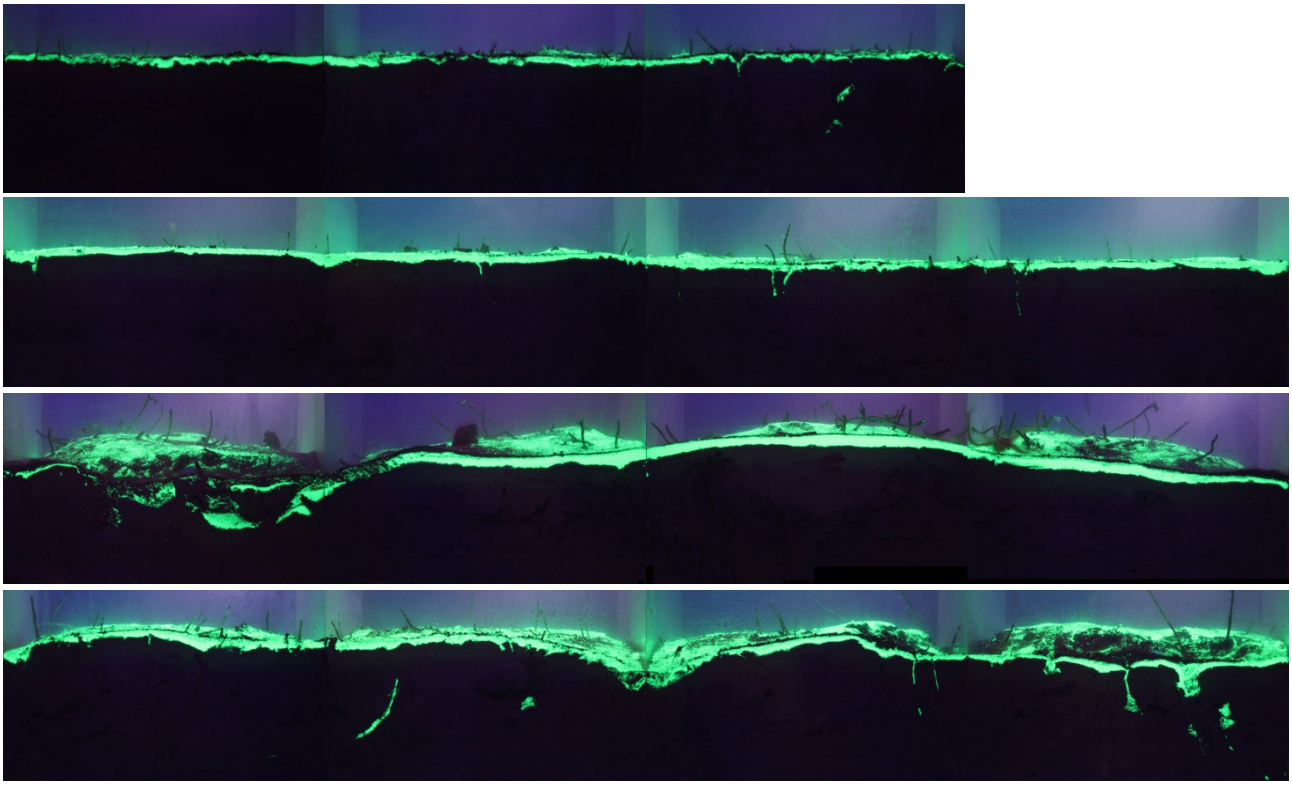

Figure S7: Replicate (n=4) f-SPI images for (a) 2017 and (b) 2018 from station B15. The images (four aquarium sides are stitched together) are presented. The green coloration is the luminophore tracer.

(a)

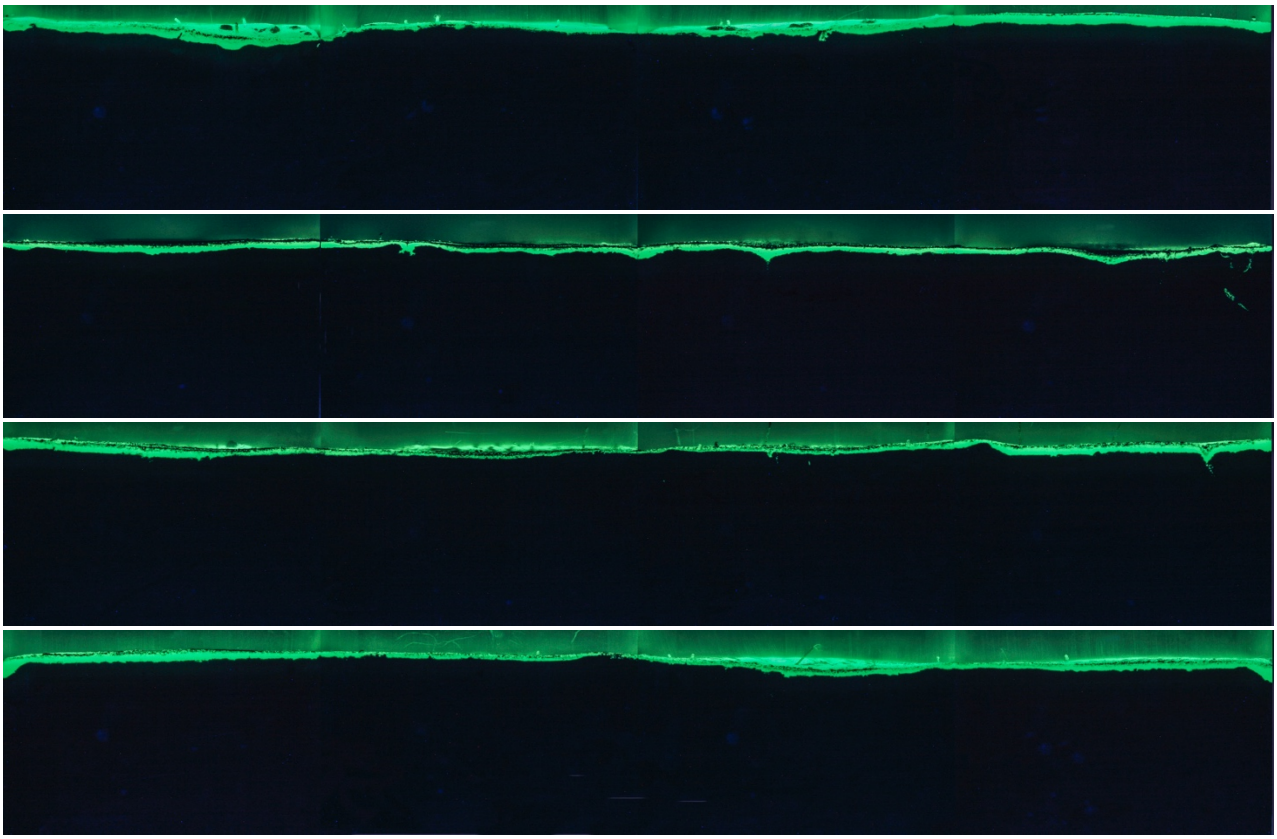

(b)

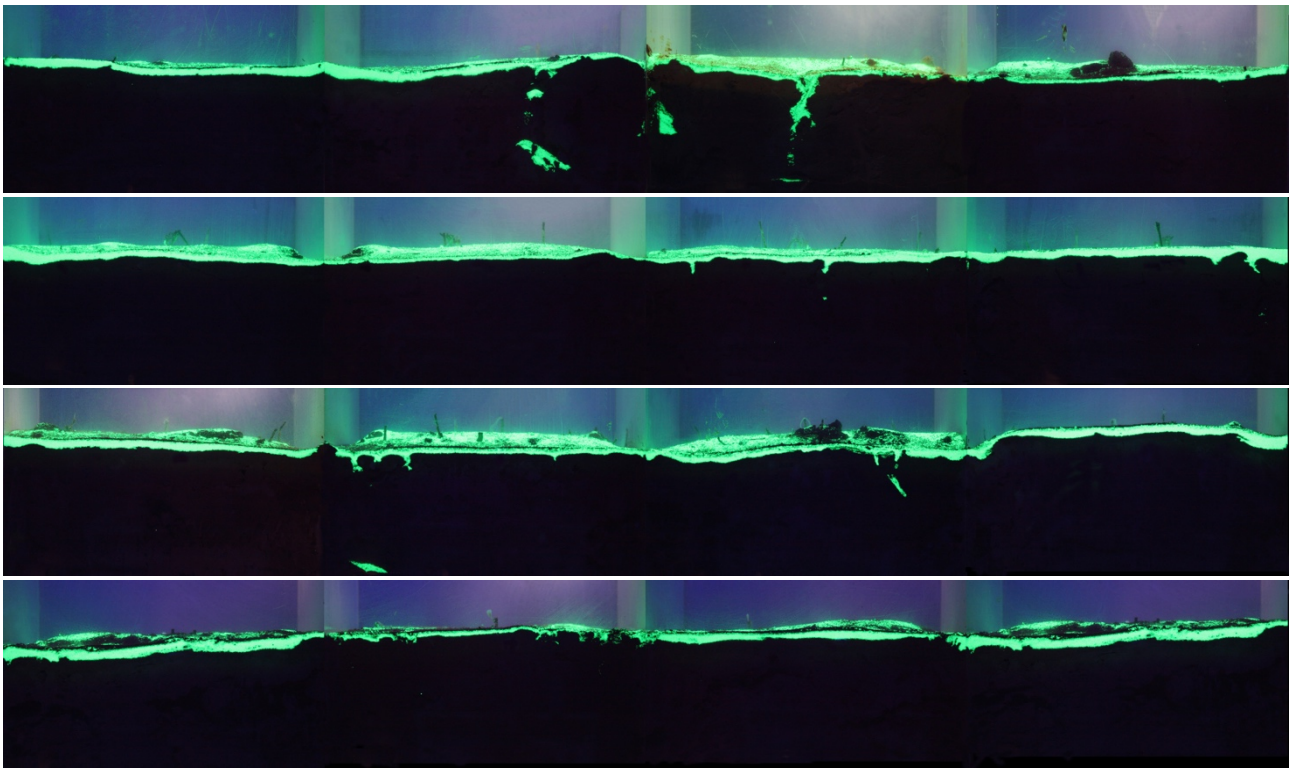

Figure S8: Replicate (n=4) f-SPI images for (a) 2017 and (b) 2018 from station B16. The images (four aquarium sides are stitched together) are presented. The green coloration is the luminophore tracer.

(a)

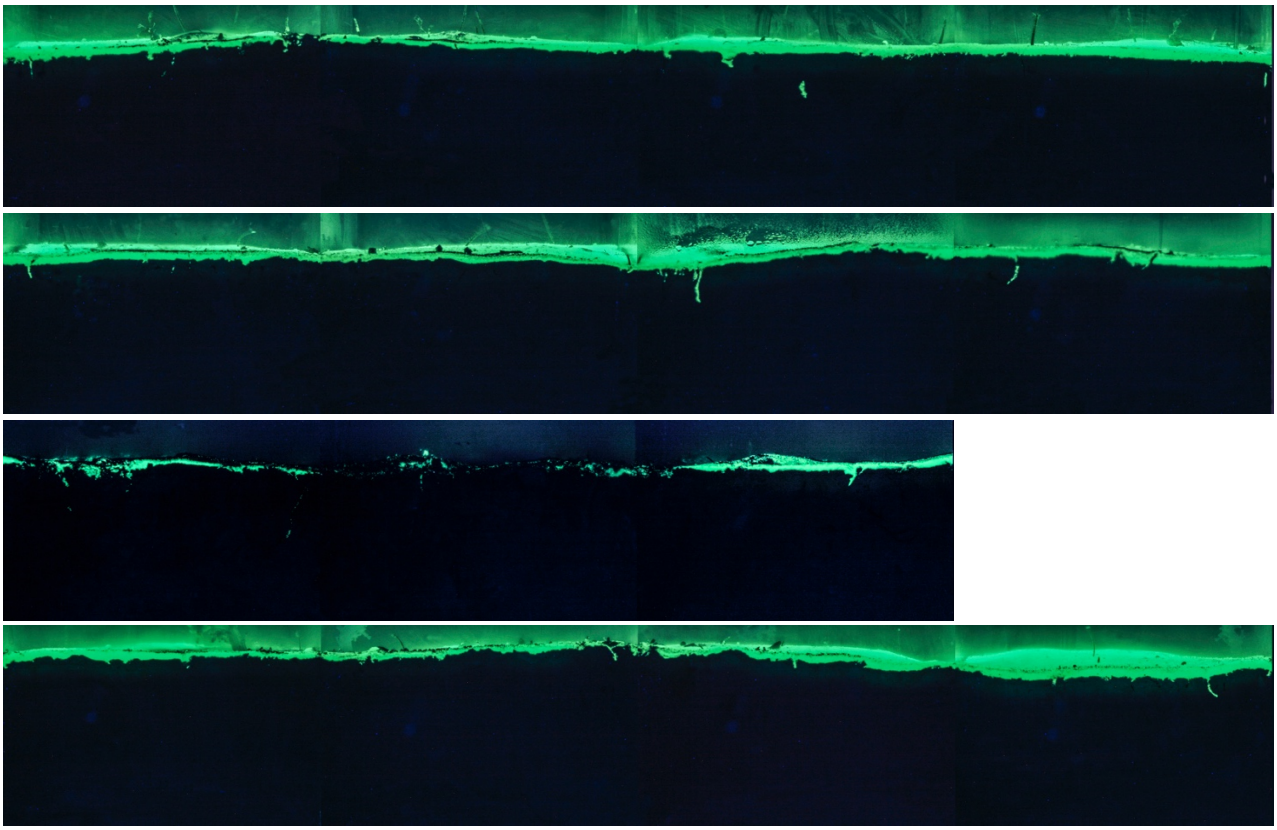

(b)

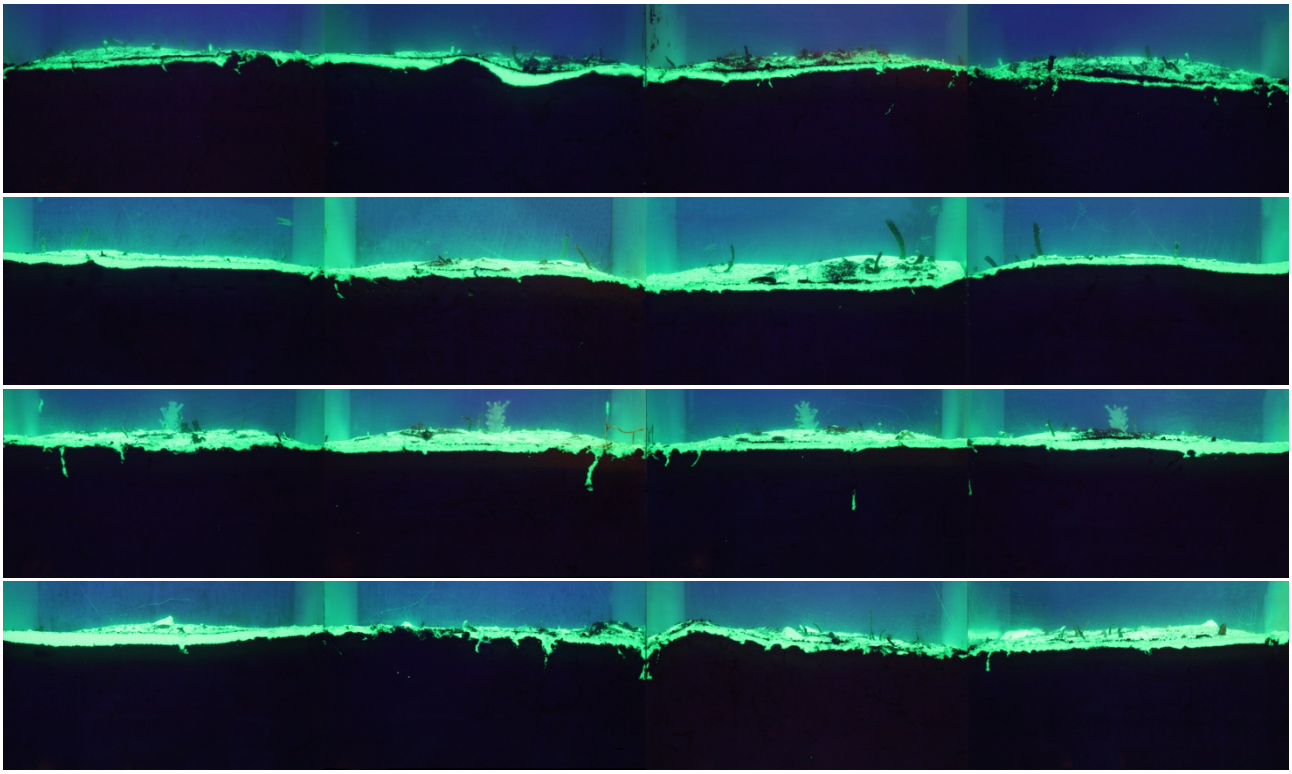

Figure S9: Replicate (n=4) f-SPI images for (a) 2017 and (b) 2018 from station B17. The images (four aquarium sides are stitched together) are presented. The green coloration is the luminophore tracer.

(a)

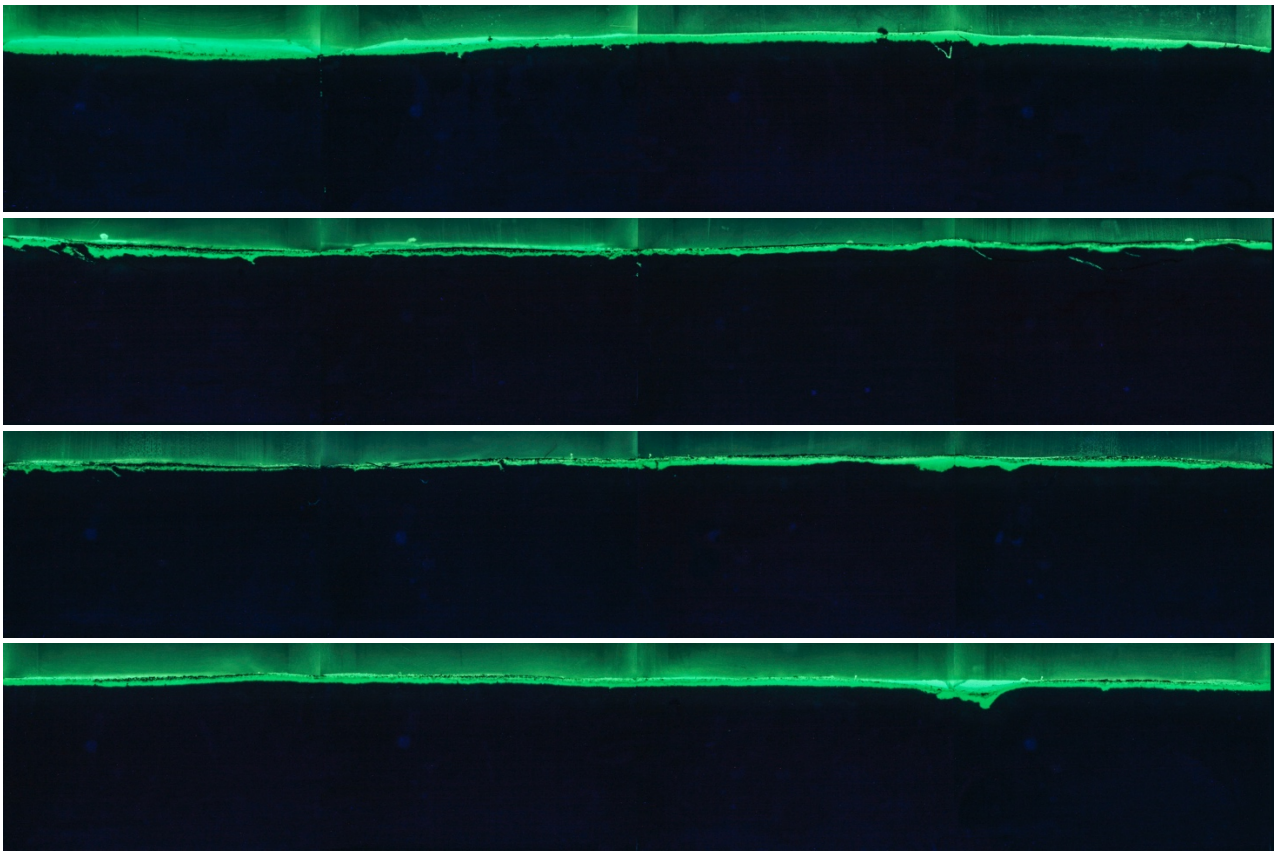

(b)

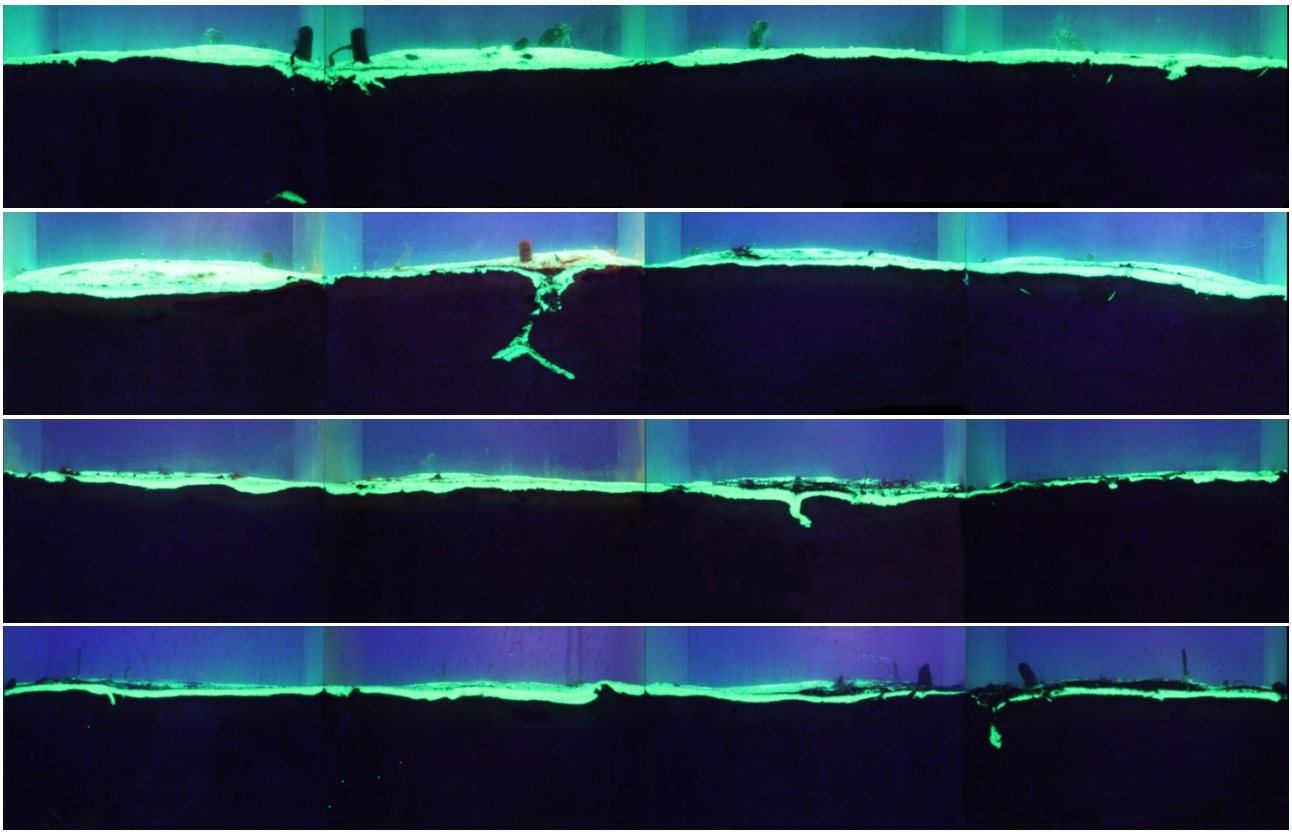

Figure S10: Replicate (n=4) f-SPI images for 2018 from station X_s. The images (four aquarium sides are stitched together) are presented. The green coloration is the luminophore tracer.

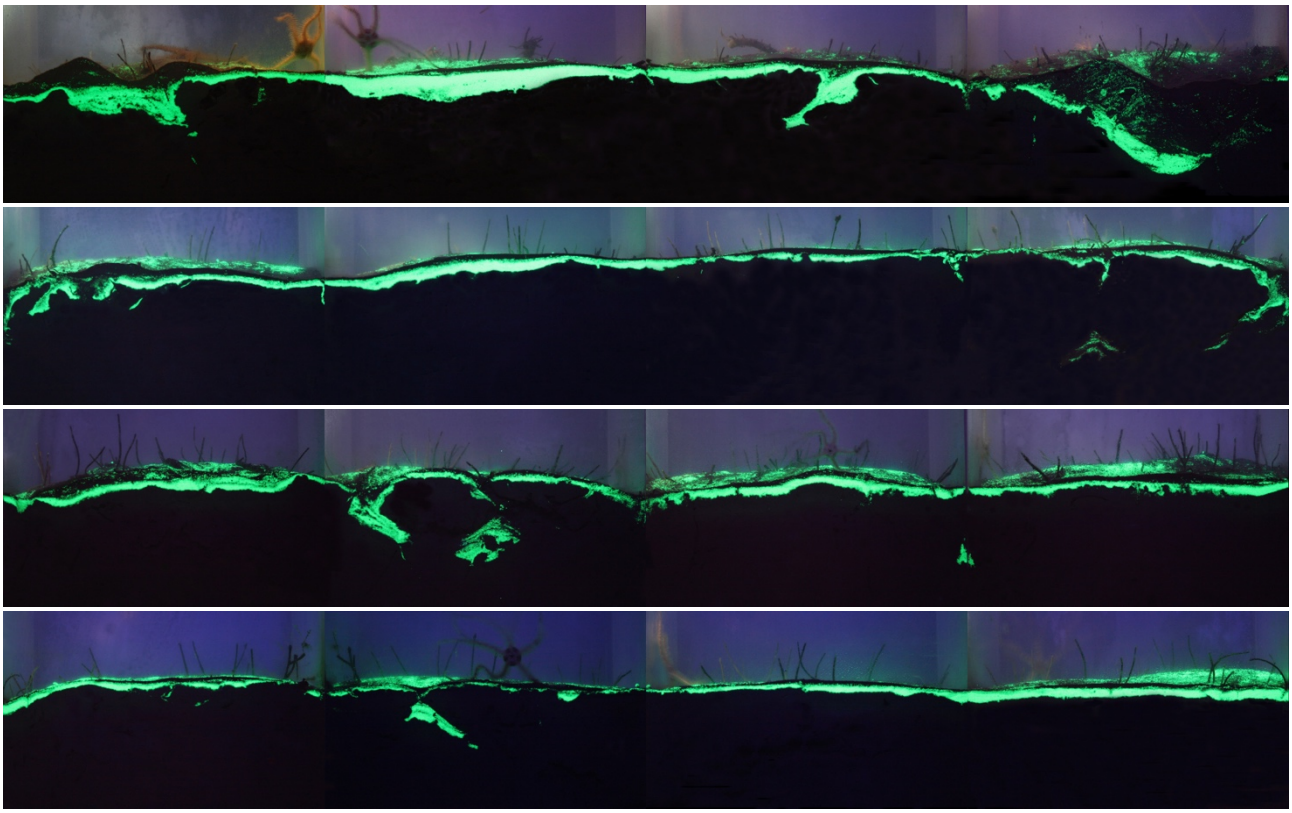

Figure S11: Sediment particle reworking profiles (n=4) derived from the 2017 f-SPI images for stations (a) B13, (b) B14, (c) B15, (d) B16 and (e) B17. Insets show detail of main figure.

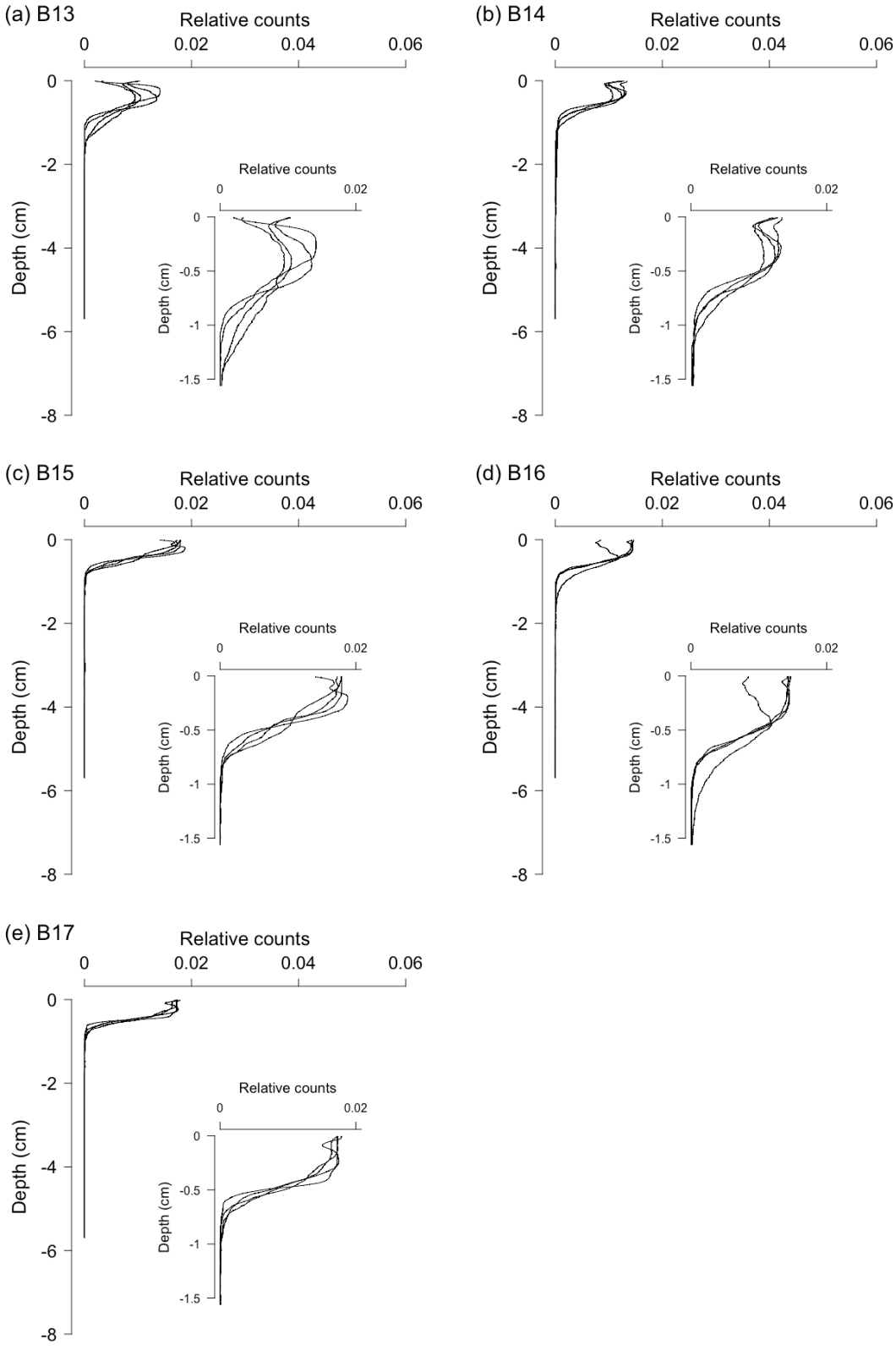

Figure S12: Sediment particle reworking profiles (n=4) derived from the 2018 f-SPI images for stations (a) B13, (b) B14, (c) B15, (d) B16, (e) B17 and (f) X_s. Insets show detail of main figure.

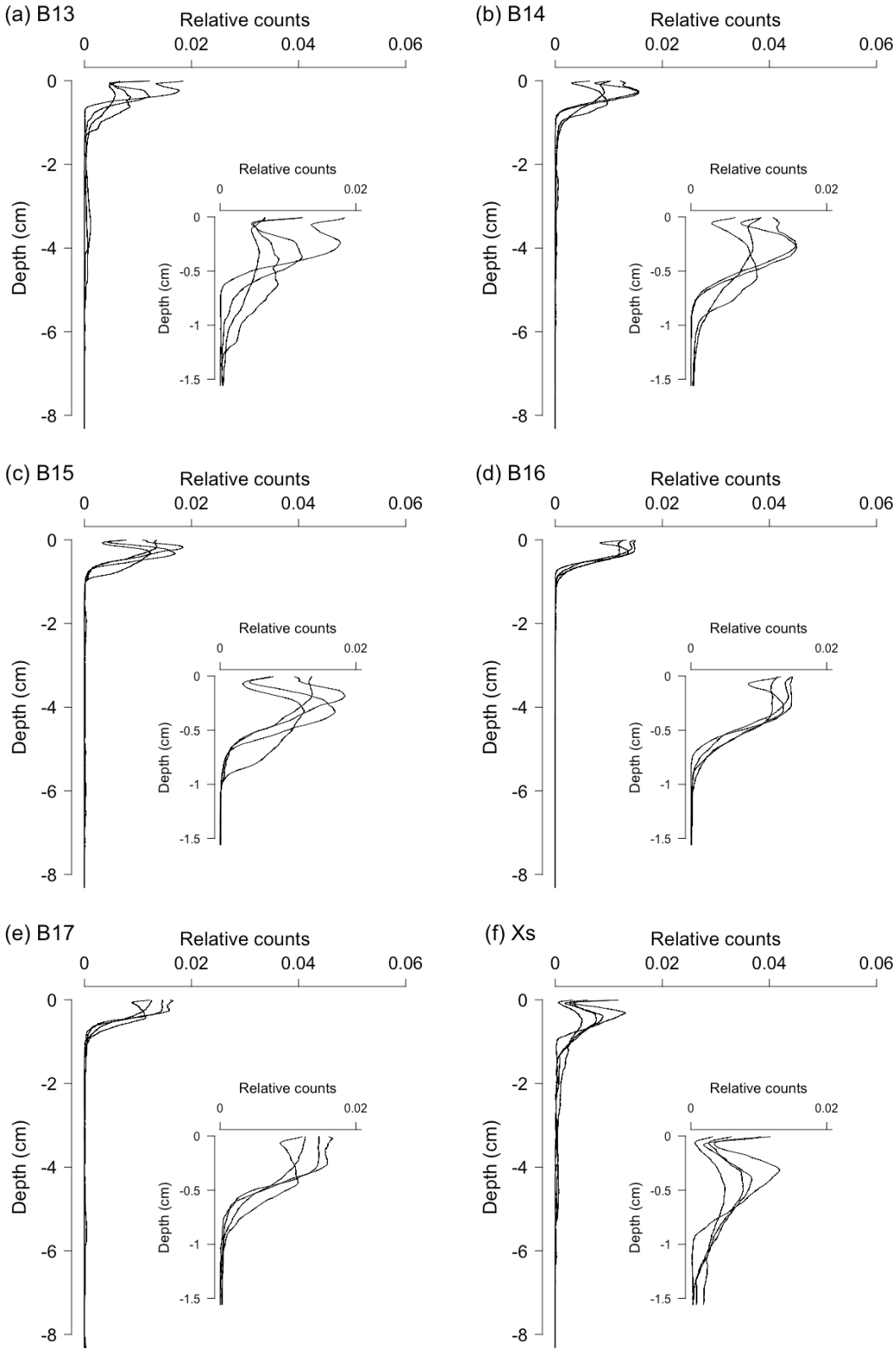

Figure S13: Cumulative sediment particle size distributions (n = 4) for stations (a) B13, (b) B14, (c) B15, (d) B16, and (e) B17 in 2017.

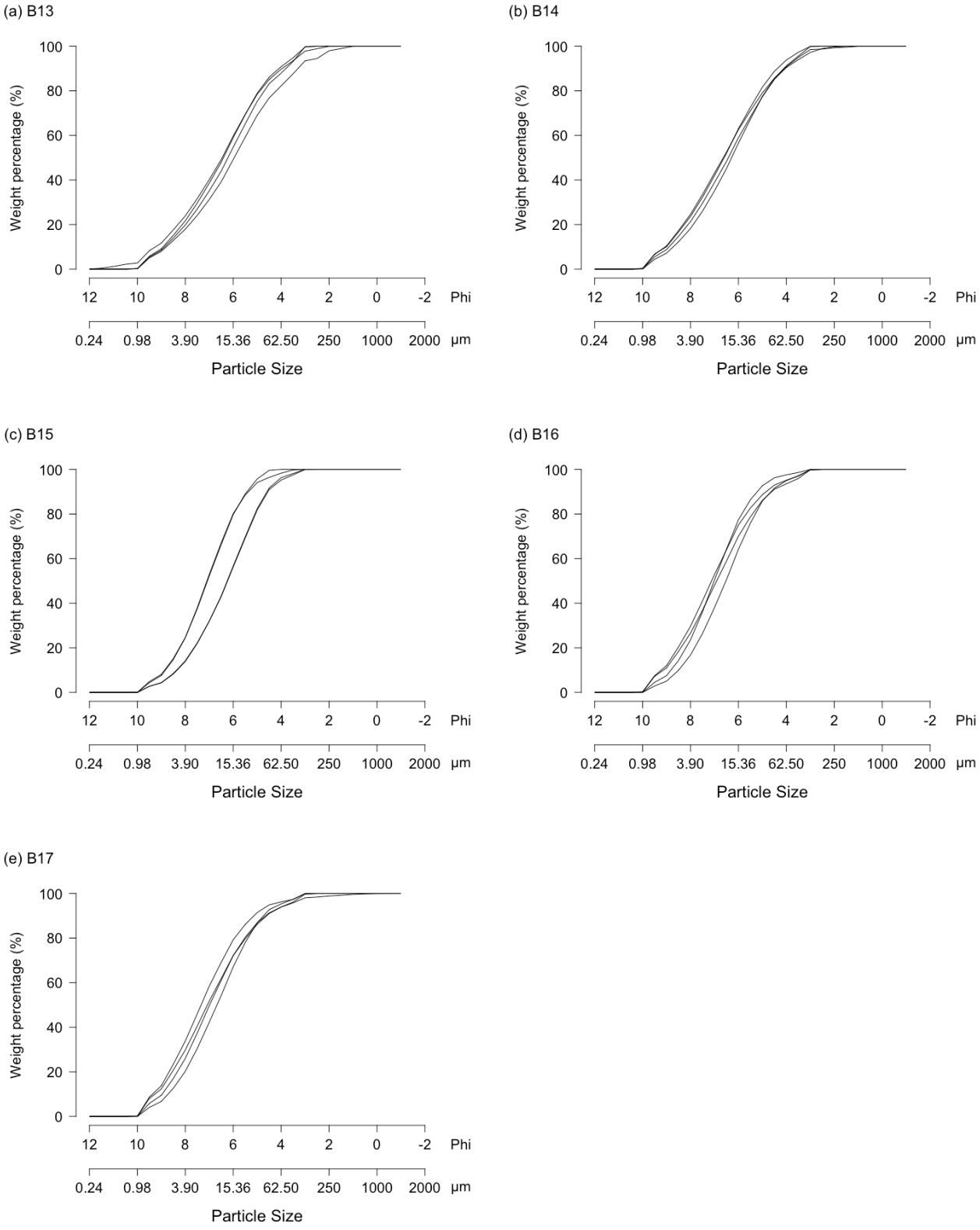

Figure S14: Cumulative sediment particle size distributions (n = 4) for stations (a) B13, (b) B14, (c) B15, (d) B16, (e) B17 and (f) Xs in 2018.

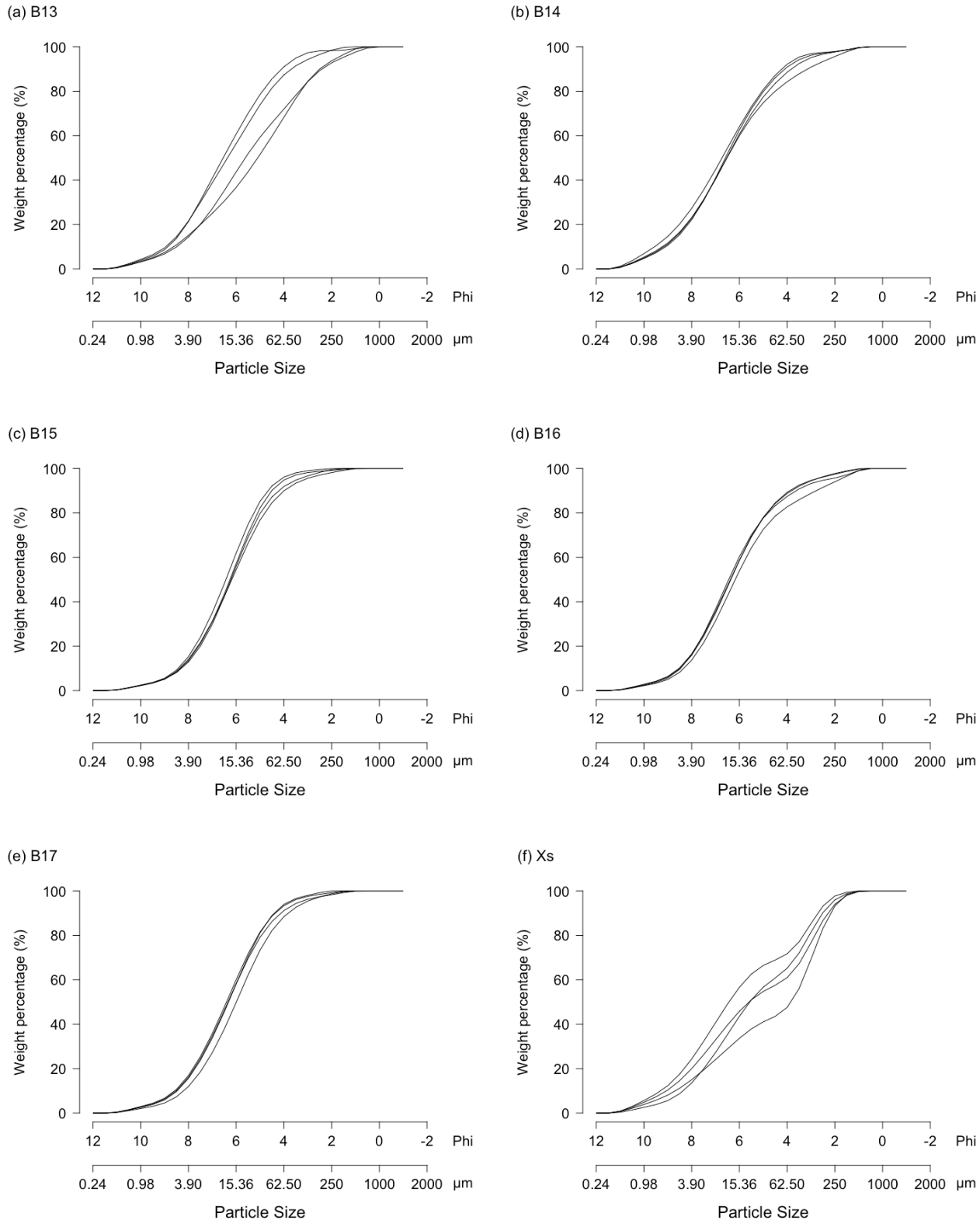

Table S3: Summary of sediment particle size statistics for each replicate core (retrieved as per Figure S3) given by the default GRADISTAT output (Blott & Pye, 2001). Mean, sorting, skewness, kurtosis, the percentage of sample less than 63 μm and total organic material are presented for all stations in (a) 2017 and (b) 2018. Superscripts provide descriptive terminology as outlined by Blott & Pye (2001). **Mean, $\bar{x}$:** fs, fine silt; ms, medium silt; cs, coarse silt; vcs, very coarse silt. **Sorting, σ:** ps, poorly sorted; vps, very poorly sorted. **Skewness, *Sk*:** sy, symmetrical; vfsk, very fine skewed; fsk, fine skewed; csk, coarse skewed. **Kurtosis, *K*:** mk, mesokurtic; lk, leptokurtic; pk, platykurtic. Organic material is by loss on ignition.

(a)

Station	Event number	Mean ($\bar{x}$, μm)	Sorting (σ, μm)	Skewness (Sk, μm)	Kurtosis (K, μm)	Sample <63 μm (%)	Organic material (%)	Sediment name
JCR16006								
B13	331	22.27^{ms}	27.28^{ps}	2.080^{sy}	7.131^{mk}	90.902	6.777	Medium silt
B13	332	24.47^{ms}	35.53^{ps}	2.993^{sy}	14.17^{mk}	89.783	7.205	Very fine sandy medium silt
B13	333	40.47^{cs}	66.83^{vps}	3.426^{sy}	17.12^{mk}	82.298	6.229	Very fine sandy coarse silt
B13	334	25.12^{ms}	29.33^{ps}	1.743^{sy}	5.276^{mk}	88.010	6.748	Very fine sandy coarse silt
B14	318	24.07^{ms}	42.88^{ps}	5.599^{sy}	46.73^{mk}	90.859	7.883	Medium silt
B14	319	25.05^{ms}	36.85^{ps}	3.373^{sy}	18.09^{mk}	90.544	7.769	Medium silt
B14	320	22.78^{ms}	26.00^{ps}	1.938^{sy}	6.512^{mk}	91.295	8.305	Medium silt
B14	321	19.17^{ms}	23.04^{ps}	2.173^{sy}	7.963^{mk}	93.866	8.354	Medium silt
B15	286	11.61^{fs}	13.40^{ps}	3.240^{sy}	16.93^{mk}	98.361	5.979	Fine silt
B15	287	10.52^{fs}	9.177^{ps}	1.644^{sy}	5.819^{mk}	100.00	7.057	Fine silt
B15	288	19.43^{ms}	19.58^{ps}	2.288^{fsk}	9.670^{mk}	96.329	7.413	Coarse silt
B15	289	20.09^{ms}	20.88^{ps}	2.252^{sy}	8.854^{mk}	95.281	7.486	Coarse silt
B16	200	14.98^{fs}	21.53^{ps}	2.965^{sy}	12.34^{mk}	95.196	7.057	Fine silt
B16	201	17.34^{ms}	24.04^{ps}	2.629^{sy}	9.934^{mk}	93.603	7.000	Medium silt
B16	203	12.87^{fs}	16.27^{ps}	3.610^{sy}	19.15^{mk}	97.598	7.077	Medium silt
B16	205	18.25^{ms}	21.76^{ps}	2.730^{sy}	11.62^{mk}	95.033	7.713	Medium silt
B17	227	16.99^{ms}	20.86^{ps}	2.745^{sy}	11.48^{mk}	95.347	7.292	Medium silt
B17	228	22.11^{ms}	63.42^{ps}	9.544^{sy}	121.8^{mk}	93.967	6.960	Fine silt
B17	229	16.70^{fs}	24.12^{ps}	2.732^{sy}	10.77^{mk}	93.975	6.739	Fine silt
B17	230	12.97^{fs}	19.82^{ps}	3.434^{sy}	15.86^{mk}	96.231	5.926	Fine silt

(b)

Station	Event number	Mean ($\bar{x}$, μm)	Sorting (σ, μm)	Skewness (Sk, μm)	Kurtosis (K, μm)	Sample <63 μm (%)	Organic material (%)	Sediment name
JCR17007								
B13	289	71.71^{cs}	127.9^{vps}	3.302^{sy}	15.83^{mk}	72.101	6.741	Very fine sandy medium silt
B13	291	29.38^{ms}	72.17^{ps}	6.785^{sy}	56.59^{mk}	91.109	6.965	Medium silt
B13	292	69.21^{cs}	103.2^{vps}	2.745^{fsk}	11.54^{mk}	68.472	6.599	Very fine sandy very coarse silt
B13	293	32.08^{ms}	54.85^{vps}	3.622^{sy}	19.08^{mk}	87.455	6.747	Very fine sandy medium silt
B14	237	32.26^{ms}	68.92^{vps}	4.915^{sy}	31.73^{mk}	88.623	7.331	Very fine sandy medium silt
B14	238	29.24^{ms}	65.98^{ps}	5.474^{sy}	38.01^{mk}	90.956	7.860	Medium silt
B14	239	42.56^{ms}	86.35^{vps}	3.551^{csk}	17.04^{lk}	84.337	7.329	Very fine sandy medium silt
B14	240	27.27^{ms}	65.03^{vps}	5.785^{sy}	41.38^{mk}	92.235	7.367	Medium silt
Xs	270	74.16^{cs}	98.00^{vps}	1.860^{sy}	7.039^{pk}	61.053	4.232	Fine sandy fine silt
Xs	271	92.26^{vcs}	96.04^{vps}	1.238^{vfsk}	4.456^{pk}	47.666	4.469	Medium silty fine sands
Xs	272	49.97^{ms}	74.33^{vps}	2.169^{csk}	8.796^{pk}	71.755	4.488	Very fine sandy fine silt
Xs	273	64.38^{cs}	84.72^{vps}	2.002^{sy}	7.744^{pk}	65.287	5.111	Very fine sandy medium silt
B15	205	23.29^{ms}	41.62^{ps}	6.901^{sy}	65.19^{mk}	94.847	6.476	Medium silt
B15	206	25.75^{ms}	39.47^{ps}	4.095^{sy}	24.40^{lk}	91.985	6.541	Medium silt
B15	207	18.88^{ms}	24.91^{ps}	4.749^{sy}	37.04^{mk}	96.165	6.659	Medium silt
B15	208	31.11^{ms}	57.70^{ps}	4.758^{sy}	30.58^{mk}	90.037	6.800	Very fine sandy medium silt
B16	189	33.29^{ms}	69.49^{ps}	4.736^{sy}	29.43^{lk}	89.361	5.643	Very fine sandy medium silt
B16	190	32.66^{ms}	64.63^{ps}	4.509^{sy}	27.51^{lk}	88.799	6.229	Very fine sandy medium silt
B16	191	51.71^{cs}	102.0^{vps}	3.276^{csk}	14.27^{lk}	82.795	6.231	Very fine sandy medium silt
B16	192	40.31^{ms}	91.13^{ps}	4.174^{csk}	21.56^{lk}	87.475	6.024	Very fine sandy medium silt
B17	134	28.46^{ms}	55.14^{ps}	5.079^{sy}	34.27^{mk}	91.254	6.250	Medium silt
B17	135	22.01^{ms}	29.75^{ps}	3.682^{sy}	20.59^{mk}	94.024	6.101	Medium silt
B17	136	23.49^{ms}	40.14^{ps}	5.252^{sy}	39.00^{mk}	93.434	6.209	Medium silt
B17	137	32.07^{ms}	50.59^{ps}	4.045^{sy}	23.70^{mk}	88.540	6.271	Very fine sandy coarse silt

Table S4: Summary of mean (± SD) community parameters (SR, species richness; J, evenness; TA, total abundance; TB, total biomass (g)) aquarium^{-1} for (a) all stations by year and (b) based on the collated dataset, with summed totals provided in square brackets. Total biomass includes taxon specific debris. SR is based on the returns for biomass and J is based on the returns for abundance.

(a)	**2017**						**2018**					
n = 4	**B13**	**B14**	**B15**	**B16**	**B17**		**B13**	**B14**	**Xs**	**B15**	**B16**	**B17**
SR	12.00 (5.23)	16.25 (2.63)	14.25 (2.63)	33.25 (4.03)	23.75 (3.95)		12.00 (6.38)	12.00 (2.16)	17.50 (9.85)	16.00 (6.00)	19.25 (9.74)	22.75 (8.42)
J	0.88 (0.14)	0.65 (0.08)	0.93 (0.02)	0.75 (0.07)	0.84 (0.05)		0.72 (0.18)	0.53 (0.16)	0.53 (0.21)	0.91 (0.03)	0.79 (0.05)	0.79 (0.07)
TA	18.75 (10.87)	49.00 (11.46)	23.50 (6.61)	148.75 (38.11)	98.25 (20.61)		32.25 (21.23)	49.00 (21.24)	100.75 (60.79)	29.25 (12.50)	100.75 (36.75)	88.00 (41.35)
TB (g)	0.99 (0.68)	1.32 (0.86)	0.15 (0.04)	2.86 (1.79)	0.39 (0.26)		1.30 (1.34)	0.61 (0.21)	1.10 (0.54)	0.18 (0.02)	0.75 (0.20)	1.12 (0.78)

(b)	**2017+2018**						
B13-B17, n = 8 Xs, n = 4	**B13**	**B14**	**Xs**	**B15**	**B16**	**B17**	**Grand total**
SR	12.00 (5.40) [54]	14.13 (3.18) [51]	17.50 (9.85) [45]	15.13 (4.39) [59]	26.25 (10.18) [85]	23.25 (6.11) [74]	157
J	0.80 (0.17) [-]	0.59 (0.13) [-]	0.53 (0.21) [-]	0.92 (0.03) [-]	0.77 (0.06) [-]	0.82 (0.06) [-]	-
TA	25.50 (17.20) [204]	49.00 (15.80) [392]	100.75 (60.79) [403]	26.38 (9.75) [211]	124.75 (43.12) [998]	93.13 (30.74) [745]	2953
TB (g)	1.15 (0.99) [9.17]	0.96 (0.69) [7.69]	1.10 (0.54) [4.39]	0.17 (0.04) [1.32]	1.81 (1.63) [14.46]	0.76 (0.66) [6.05]	43.0935

Figure S15: Summary of diagnostics for ordination showing (a-b) group polygons by station, (c,d) Shepard goodness of fit (R^2) between dissimilarities and fitted distances, and (e,f) goodness of fit measure for individual observations within the visualization based on faunal (a,c,e) abundance and (b,d,f) biomass.

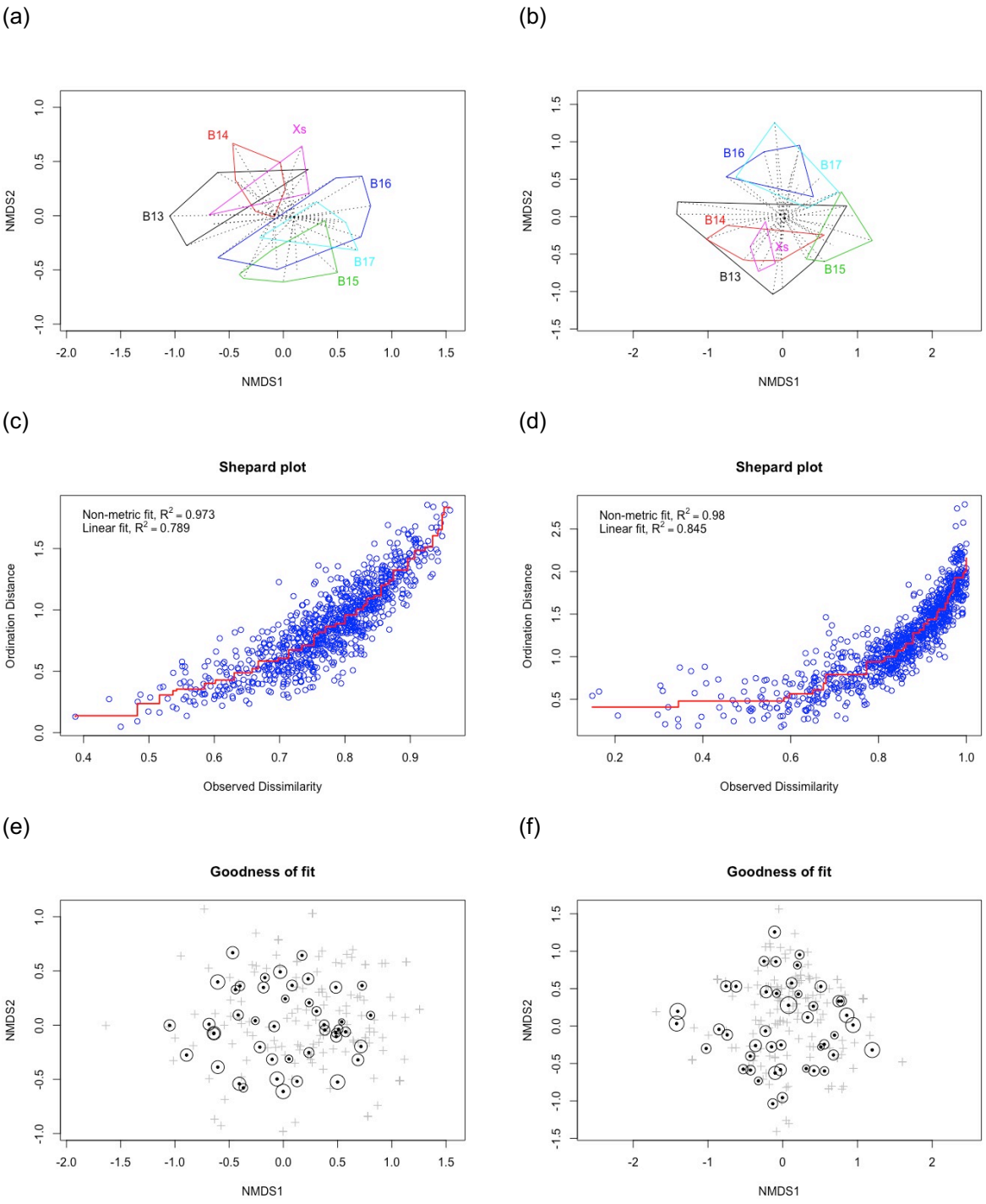

Table S5: Summary of the species (or higher taxa) that collectively contribute approximately half of the contribution to overall dissimilarity ($\sum S_i$ ~50%, indicated for each pairwise contrast) between stations based on (a) abundance and (b) biomass with taxa listed in rank order (most to least) of average contribution to dissimilarity. Font colour indicates a positive (green) versus negative (red) directional change in (a) mean abundance or (b) mean biomass representation between each station pair (row relative to column, i.e. green indicates y > x, red indicates y < x).

(a)	B13	B14	Xs	B15	B16
B14	*Spiochaetopterus typicus* *Lumbrineris mixochaeta* *Maldane sarsi* Nemertea *Nephtys incisa* *Spiophanes kroyeri* *Haploops tubicola* *Ctenodiscus crispatus* *Chaetozone setosa* *Scutopus ventrolineatus* Yoldiidae *Adontorhina* juv. *Antalis entalis* *Nephasoma procera* Nematoda (51.65%)	-			
Xs	*Spiochaetopterus typicus* Yoldiidae *Lumbrineris mixochaeta* *Owenia polaris* *Adontorhina* juv. *Spiophanes kroyeri* *Chaetozone setosa* *Levinsenia gracillis* *Leitoscoloplos mammosus* *Ctenodiscus crispatus* *Maldane sarsi* (50.41%)	Yoldiidae *Spiochaetopterus typicus* *Owenia polaris* *Maldane sarsi* *Adontorhina* juv. *Spiophanes kroyeri* *Lumbrineris mixochaeta* *Leitoscoloplos mammosus* Nemertea *Nephtys incisa* *Levinsenia gracillis* *Scutopus ventrolineatus* *Ctenodiscus crispatus* *Nephasoma procera* (52.02%)	-		
B15	*Spiochaetopterus typicus* *Spiophanes kroyeri* *Maldane sarsi* *Nephasoma procera* Nematoda Yoldiidae *Abyssoninoe hibernica* *Lumbrineris mixochaeta* *Haploops tubicola*	*Spiochaetopterus typicus* *Spiophanes kroyeri* Nematoda *Lumbrineris mixochaeta* *Nephasoma procera* Yoldiidae Nemertea *Nephtys incisa* *Maldane sarsi*	*Spiochaetopterus typicus* Yoldiidae *Spiophanes kroyeri* *Maldane sarsi* *Owenia polaris* Nematoda *Lumbrineris mixochaeta* *Nephasoma procera* *Adontorhina* juv.	-	

	Chaetozone setosa *Ophelina abranchiata* *Mediomastus fragilis* *Nephtys incisa* *Ctenodiscus crispatus* (50.84%)	*Abyssoninoe hibernica* *Ctenodiscus crispatus* *Scutopus ventrolineatus* *Haploops tubicola* (51.62%)	*Leitoscoloplos mammosus* *Abyssoninoe hibernica* (51.98%)		
B16	*Maldane sarsi* Yoldiidae *Spiochaetopterus typicus* *Chirimia biceps* *Nephasoma procera* *Spiophanes kroyeri* *Haploops tubicola* *Lumbrineris mixochaeta* Nematoda *Leitoscoloplos mammosus* *Mediomastus fragilis* *Levinsenia gracillis* (51.67%)	*Maldane sarsi* *Spiochaetopterus typicus* Yoldiidae *Chirimia biceps* *Haploops tubicola* *Nephasoma procera* *Spiophanes kroyeri* Nematoda *Leitoscoloplos mammosus* *Lumbrineris mixochaeta* *Levinsenia gracillis* *Mediomastus fragilis* (51.59%)	*Spiochaetopterus typicus* *Maldane sarsi* Yoldiidae *Chirimia biceps* *Haploops tubicola* *Spiophanes kroyeri* *Nephasoma procera* *Owenia polaris* *Adontorhina* juv. Nematoda *Lumbrineris mixochaeta* (50.54%)	*Maldane sarsi* Yoldiidae *Chirimia biceps* *Haploops tubicola* *Spiophanes kroyeri* *Lumbrineris mixochaeta* *Nephasoma procera* *Leitoscoloplos mammosus* Nematoda *Spiochaetopterus typicus* *Mediomastus fragilis* *Levinsenia gracillis* *Chaetozone setosa* *Glyphanostomum pallescens* *Abyssoninoe hibernica* (51.14%)	-
B17	*Nephasoma procera* *Maldane sarsi* *Spiochaetopterus typicus* *Adontorhina* juv. *Lumbrineris mixochaeta* *Leitoscoloplos mammosus* Nematoda *Thyasira equalis* *Chirimia biceps* *Mediomastus fragilis* Yoldiidae *Ophelina abranchiata* (51.52%)	*Spiochaetopterus typicus* *Nephasoma procera* *Maldane sarsi* *Adontorhina* juv. *Leitoscoloplos mammosus* Nematoda *Thyasira equalis* *Chirimia biceps* *Mediomastus fragilis* Yoldiidae *Ophelina abranchiata* (50.01%)	*Spiochaetopterus typicus* *Nephasoma procera* *Maldane sarsi* *Adontorhina* juv. Yoldiidae Nematoda *Owenia polaris* *Thyasira equalis* *Chirimia biceps* *Mediomastus fragilis* *Leitoscoloplos mammosus* (50.21%)	*Nephasoma procera* *Adontorhina* juv. *Leitoscoloplos mammosus* *Maldane sarsi* *Lumbrineris mixochaeta* *Spiophanes kroyeri* *Thyasira equalis* *Chirimia biceps* *Mediomastus fragilis* *Spiochaetopterus typicus* Nematoda Yoldiidae *Ophelina abranchiata* *Chaetozone setosa* (50.07%)	Yoldiidae *Maldane sarsi* *Adontorhina* juv. *Haploops tubicola* *Nephasoma procera* *Spiophanes kroyeri* *Chirimia biceps* Nematoda *Mediomastus fragilis* *Thyasira equalis* *Ophelina abranchiata* *Lumbrineris mixochaeta* *Levinsenia gracillis* *Leitoscoloplos mammosus* *Chaetozone setosa* *Heteromastus filiformis* *Spiochaetopterus typicus* (50.67%)

(b)	B13	B14	Xs	B15	B16
B14	*Ctenodiscus crispatus* *Spiochaetopterus typicus* *Bathyarca glacialis* (56.07%)	-			
Xs	*Ctenodiscus crispatus* *Spiochaetopterus typicus* *Nephtys incisa* (54.69%)	*Spiochaetopterus typicus* *Ctenodiscus crispatus* *Nephtys incisa* *Aglaophamus malmgreni* (54.85%)	-		
B15	*Ctenodiscus crispatus* *Spiochaetopterus typicus* *Bathyarca glacialis* (50.56%)	*Spiochaetopterus typicus* *Ctenodiscus crispatus* *Astarte crenata agg* (55.27%)	*Spiochaetopterus typicus* *Nephtys incisa* *Aglaophamus malmgreni* (56.57%)	-	
B16	*Ctenodiscus crispatus* *Astarte crenata agg* *Maldane sarsi* *Chirimia biceps* (56.00%)	*Astarte crenata agg* *Ctenodiscus crispatus* *Spiochaetopterus typicus* (50.66%)	*Spiochaetopterus typicus* *Astarte crenata* agg. *Maldane sarsi* *Ctenodiscus crispatus* (54.28%)	*Astarte crenata* agg. *Maldane sarsi* *Chirimia biceps* *Ctenodiscus crispatus* (54.10%)	-
B17	*Ctenodiscus crispatus* *Spiochaetopterus typicus* *Aglaophamus malmgreni* *Chirimia biceps* *Amphitrite groenlandica* (51.72%)	*Spiochaetopterus typicus* *Ctenodiscus crispatus* *Aglaophamus malmgreni* *Chirimia biceps* *Nephtys incisa* (55.98%)	*Spiochaetopterus typicus* *Nephtys incisa* *Aglaophamus malmgreni* *Amphitrite groenlandica* (51.32%)	*Aglaophamus malmgreni* *Chirimia biceps* *Amphitrite groenlandica* *Ctenodiscus crispatus* *Spiochaetopterus typicus* Nemertea *Maldane sarsi* (52.28%)	*Astarte crenata* agg. *Ctenodiscus crispatus* *Maldane sarsi* *Chirimia biceps* *Amphitrite groenlandica* (52.81%)

Table S6: Summary of biodiffusion coefficient (Db, $cm^2\,year^{-1}$) values determined for the vertical distribution of luminophore particles for each replicate aquarium at each station across both years.

		Station					
Year	**Replicate**	**B13**	**B14**	**Xs**	**B15**	**B16**	**B17**
2017	1	4.362	4.989	-	2.199	2.735	1.941
	2	4.209	3.077	-	1.776	2.658	1.915
	3	9.153	4.019	-	1.964	5.811	2.073
	4	6.631	3.859	-	1.748	2.607	1.768
	x̄:	**6.089**	**3.986**	-	**1.922**	**3.453**	**1.924**
	SD:	**2.324**	**0.785**	-	**0.208**	**1.573**	**0.125**
2018	1	13.368	2.856	39.558*	2.279	3.127	2.001
	2	4.658	2.271	10.593	1.927	1.951	2.906
	3	1.677	7.420	11.523	3.207	2.178	1.711
	4	7.905	5.328	5.128	5.484	2.943	3.863
	x̄:	**6.902**	**4.469**	**16.700**	**3.224**	**2.550**	**2.621**
	SD:	**5.005**	**2.372**	**15.497**	**1.600**	**0.573**	**0.972**

*includes extensive gallery and mounding by a single individual of the amphipod *Quasimelita quadrispinosa* (see Figure S16 and outlier in Figure 3 of the main manuscript)

Figure S16: Extensive mound and gallery formation by a single individual of the amphipod *Quasimelita quadrispinosa* (foreground, centre right) in aquarium replicate 1, Station Xs. The green coloration is the luminophore tracer (aquarium internal width = 20 cm).

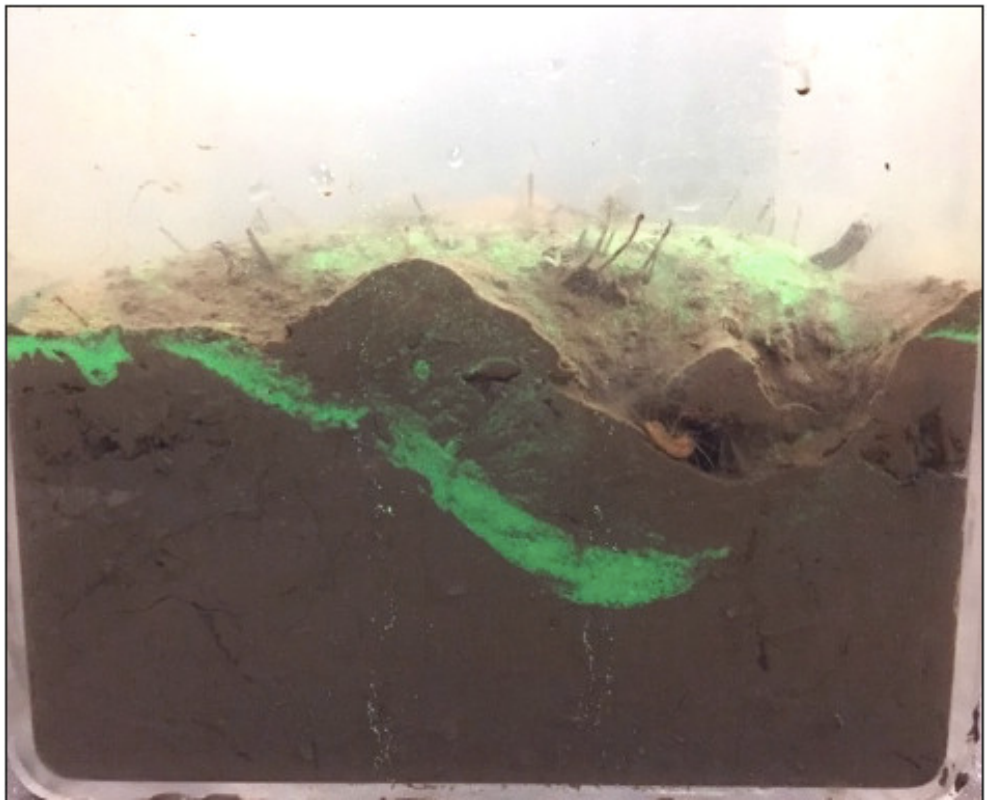

Figure S17: The effects of station and year on mean (± s.e., n = 4) organic material (loss on ignition) of surface sediments for stations B13-B17 in 2017 (black) and stations B13-B17 and Xs in 2018 (grey). Individual replicate values are presented in Table S3.

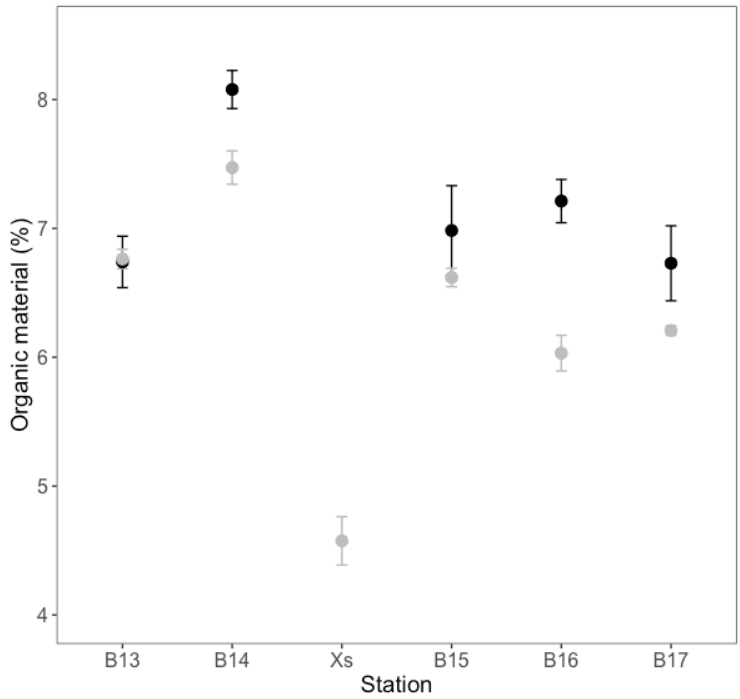

Supplementary material references

Blott SJ, Pye K. 2001. GRADISTAT: A grain size distribution and statistics package for the analysis of unconsolidated sediments. Earth Surf. Process. Landforms 26, 1237-1248 (doi: 10.10002/esp.261)

Fetterer F, Savoie M, Helfrich S, Clemente-Colón P. 2010, updated daily. Multisensor Analyzed Sea Ice Extent - Northern Hemisphere (MASIE-NH), Version 1. [Indicate subset used]. Boulder, Colorado USA. NSIDC: National Snow and Ice Data Center. (doi: https://doi.org/10.7265/N5GT5K3K) [accessed 30/01/2020].

ENDS.